CMLS, Cell. Mol. Life Sci. 62 (2005) 2112–2123
1420-682X/05/182112-12
DOI 10.1007/s00018-005-5224-y

CMLS Cellular and Molecular Life Sciences

Research Article

Nucleotide binding domains of human CFTR: a structural classification of critical residues and disease-causing mutations.

R. Eudes[a], P. Lehn[b], C. Férec[b], J.-P. Mornon[a], I. Callebaut[a, *]

[a] Département de Biologie Structurale, IMPMC, CNRS UMR7590, Universités Paris 6 et Paris 7, case 115, 4 place Jussieu, 75252 Paris Cedex 05 (France), e-mail: Isabelle.Callebaut@impmc.jussieu.fr
[b] INSERM U613, Génétique moléculaire et génétique épidémiologique, CHU de Brest, Université de Bretagne Occidentale, Brest (France)

Received 24 May 2005; received after revision 13 June 2005; accepted 18 June 2005
Online First 26 August 2005

Abstract. Defective function of the cystic fibrosis (CF) transmembrane conductance regulator (CFTR) causes CF, the most frequent lethal inherited disease among the Caucasian population. The structure of this chloride ion channel includes two nucleotide-binding domains (NBDs), whose ATPase activity controls channel gating. Recently, the experimental structures of mouse and human CFTR NBD1 and our model of the human CFTR NBD1/NBD2 heterodimer have provided new insights into specific structural features of the CFTR NBD dimer. In the present work, we provide a structural classification of CF-causing mutations which may complement the existing functional classification. Our analysis also identified amino acid residues which may play a critical role in interdomain interaction and are located at the NBD1-NBD2 interface or on the surface of the dimer. In particular, a cluster of aromatic amino acids, which includes F508 and straddles the two NBDs, might be directly involved in the interaction of the NBD1/NBD2 heterodimer with the channel-forming membrane-spanning domains.

Key words. CFTR; cystic fibrosis; nucleotide binding domain; molecular modeling; structural classification; critical residue; CF mutation; ABC transporter.

Cystic fibrosis (CF) is the most common lethal genetic disease in the Caucasian population. It is caused by mutations in the CF transmembrane conductance regulator (CFTR) gene. The CFTR protein, which is a low-conductance cAMP-dependent and ATP-gated chloride channel localized at the apical membrane of epithelial cells, belongs to the large superfamily of ATP-binding cassette (ABC) transporters [reviewed in refs. 1, 2]. It is composed of two halves, each possessing a membrane-spanning domain (MSD) and a nucleotide-binding domain (NBD, also called the ABC domain). The two halves are linked by a regulatory (R) domain, the phosphorylation of which regulates channel activity [3]. More than a thousand mutations have been described in CF patients (http://www.genet.sickkids.on.ca/cftr). Their frequency is highly variable following the geographical area but only a few of the total CF mutations are represented in over 1%. The most prevalent mutation, ΔF508 [the deletion of a phenylalanine at position 508 in the first NBD (NBD1)] accounts for approximately 70% of chromosomes in CF patients. Mutations in the CFTR gene have been classified into different groups according to the mechanism by which they disrupt CFTR function [4].

* Corresponding author.

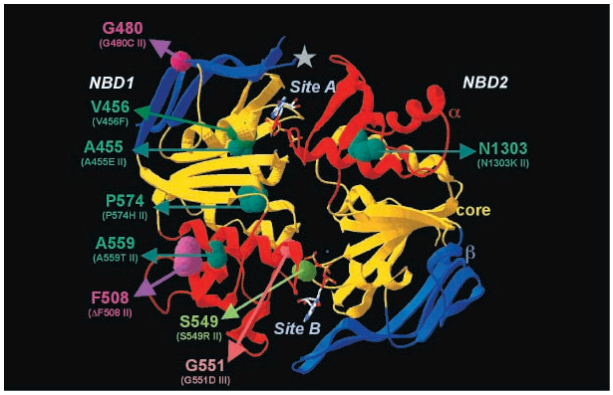

Figure 1. Ribbon representation of the human CFTR heterodimer of nucleotide-binding domains NBD1/NBD2, showing the localization of a series of amino acids involved in CF mutations which have been functionally characterized. The heterodimer is viewed from the MSDs (top view). The NBD core, α and β subdomains are shown in yellow, red and blue, respectively. The non-canonical and canonical ATP-binding sites are labeled site A and site B, respectively. The large insertion (regulatory insertion) between the first two NBD1 β strands has not been modeled and is symbolized by a gray star. The bound nucleotides are shown in space-filling representations. Missense mutations affecting A455, P574, A559, N1303, G480 and S549 are classified as class II mutations (as indicated below the corresponding residues) characterized by defective CFTR processing and maturation. The first four amino acids (dark green) are buried inside the heterodimeric structure. V456 is a buried residue located at a topohydrophobic position which has also been found mutated in CF. N1303 forms an important network of hydrogen bonds with amino acids of the γ-phosphate linker (Q-loop, see text). S549 (light green) is located within the conventional ATP-binding site B at the NBD1/NBD2 interface. F508 and G480, the deletion and substitution of which, respectively, also lead to class II mutations, are both shown in pink and are exposed on the surface of the NBD1 subunit. Most of the class III mutants (affecting Cl^- channel gating) are located within the ATP-binding sites, as exemplified here by G551D (salmon).

In particular, class II mutations (including ΔF508) affect protein maturation, leading to a lack of functional protein at the apical cell surface. On the other hand, class III mutations affect chloride channel regulation/gating, as they produce appropriately localized protein that does not correctly respond to stimulation. However, the relationship between the CFTR genotype and the heterogeneous CF disease phenotype is still not well understood. Progressive lung failure is the major cause of death, but the complex phenotype also involves the intestine, pancreas and reproductive system.

Several experimental structures of NBDs from ABC transporters have been reported, highlighting the specific architecture of this family of nucleotide hydrolases and its organization into functional homo- or heterodimers [for a review see ref. 5]. These NBDs are organized into an F1-ATPase-like catalytic core (depicted in yellow in fig. 1), bearing most of the conserved ABC motifs for ATP binding (Walker A or P-loop, Walker B, Q-loop, H-loop), which is accompanied by specific β and α subdomains. The β subdomain (blue in fig. 1) consists of a short β sheet, covering the nucleotide-binding site, and includes a conserved aromatic amino acid which provides stacking interaction with the ATP adenine ring. The α subdomain (red in fig. 1), which is the most variable among the different NBD domains, includes the Walker C motif (also called the ABC signature) and is thought to play a key role in intramolecular signal transduction. Indeed, according to the experimental three-dimensional structure of complete ABC transporters (BtuCD [6], MsbA [7, 8]), it mediates the interaction with the MSDs. As shown by the recent experimental structures of mouse and human CFTR NBD1 [9, 10] and our own model of the human CFTR NBD1/NBD2 heterodimer [11], the CFTR NBD1 and NBD2 have maintained such a general architecture with, however, some noticeable features in CFTR NBD1, especially in the β subdomain which accommodates a large insertion between its first two β strands and lacks two regular secondary structures usually present in ABC NBDs (fig. 1).

Several three-dimensional experimental structures also revealed a head-to-tail arrangement of the two NBDs, in which the nucleotide is sandwiched between the two subunits, each nucleotide-binding site being formed by the Walker A, Walker B, Q-loop and switch motifs of one subunit and by the Walker C motif of the other subunit [6, 12, 13]. Such an arrangement with the ATP active sites at the interface between the two NBDs is in agreement with the ATP switch model for ABC transporters in which ATP binding and ATP hydrolysis induce formation and dissociation, respectively, of the NBD dimer, thereby providing a switch inducing conformational changes in the MSDs [14]. Our recent model of the three-dimensional structure of the human CFTR NBD1/NBD2 heterodimer is also characterized by such a head-to-tail configuration [11] with an asymmetry of the two ATP-binding sites. Indeed, the canonical site (mainly contributed by NBD2 and thus termed site B), has all the amino acids necessary for ATP hydrolysis, whereas the non-canonical site (mainly formed by NBD1 and thus termed site A), lacks most of these residues. Experimental data have shown that this heterodimeric organization of the CFTR NBDs is required for optimal catalytic activity [15] and have demonstrated the functional asymmetry of the ATP-binding sites, with a rapid ATP turnover at the standard canonical site, while ATP remains bound, in the non-hydrolyzed form, for a long time at the unconventional, non-canonical site [16, 17]. Thus, it appears that normal gating requires ATP-binding at both sites and hydrolysis only at the canonical site [18].

However, despite these recent data concerning the experimental structures of mouse and human CFTR NBD1 (either wild-type [9] or with mutations/deletion of F508 [10, 19]) and our human CFTR NBD1/NBD2 heterodimer model [11], no in-depth analysis of critical amino acid

positions within these structures has yet been reported, except, to some extent, for F508 and the ABC conserved motifs. This is all the more surprising as, in contrast to some other disease-associated proteins, a large number of mutations in the CFTR NBD domains have been described in CF patients (http://www.genet.sickkids.on.ca/cftr). These mutations are localized all along the NBD sequence and can thus affect the NBD structure as well as its function. Moreover, only a few mutations have been experimentally analyzed at the molecular level, and the pathological significance of other variants may even be questionable, as some presumed missense substitutions may in fact correspond to non-pathological polymorphisms. Thus, given this highly particular context, we aimed in the present work to further analyze our heterodimer model in order to provide a structural classification of human CFTR NBD mutants, which should be complementary to the previous mechanism-based functional classification [4, 20]. Although some caution has to be taken with regard to the atomic interactions observed on the basis of a static model, analysis of the structural localization of the mutated residues may indeed give important insights into the molecular consequences of the corresponding mutations and help to interpret or predict the effects of sequence alterations that have been, or remain to be functionally characterized. Such an endeavor may significantly contribute to a better understanding of the CF genotype/phenotype relationships. In addition, our analysis also permitted us to unravel the potential role of some critical amino acids predicted to participate in interdomain interactions, either with the other NBD subunit or with the channel-forming MSDs.

Materials and methods

Using a detailed sequence/structure analysis, we have previously proposed a three-dimensional model of the human CFTR NBD1/NBD2 heterodimer [11]. In the present work, we obviously based our approach on our model but we also took into consideration the very recent data on the experimental structures of the mouse and human CFTR NBD1 [9, 10]. Interestingly, no major difference could actually be observed between our human NBD1 model and the mouse and human NBD1 experimental structures as regards the alignment of their sequences with other ABC NBD domains, except for a shift of nine amino acids in helix α_α 2 (see below). In particular, no significant differences were observed for the active-site motifs and for the NBD1 regions forming the interface with NBD2. Moreover, the large insertion between strands β_β1 and β_β2, termed the regulatory insertion (RI) [9, 10], was also correctly predicted. However, following superimposition of the experimental structures of MJ0796 [13], which we had used as template for modeling [11], and of the mouse and human CFTR NBD1 [9, 10], we could observe that an insertion and a deletion were to be made between the two sequences before and after helix α_α2, respectively (see supplementary material at http://www.lmcp.jussieu.fr/~mornon/CFTR.html). This suggests that the MJ0796 structure was in fact not the best template for modeling of the α subdomains of the CFTR NBDs. A much better superimposition of the experimental structure of mouse and human CFTR NBD1 could indeed be observed in this region with the human TAP1 structure [21] (see supplementary material at the internet website address indicated above).

We thus refined our CFTR NBD model by using for its construction two templates: MJ0796 as the major template and TAP1 for part of the subdomain α (see again supplementary material). This led to the construction of models of the CFTR NBDs in which the α_α2 helix can now be perfectly superimposed with the corresponding helix of the experimental NBD1 structures, and in which the short β sheet including strands β' and β'' is maintained, as in the experimental structures of mouse NBD1 and human TAP1 (see supplementary material at http://www.lmcp.jussieu.fr/~mornon/CFTR.html). Root mean square (r.m.s.) deviations were as follows: (i) between the observed (mouse and human) and modeled (human) CFTR NBD1 structures, r.m.s. deviations were 1.47 Å and 1.52 Å, respectively (338 and 338 superimposed Cα atoms); (ii) between the observed (mouse and human) CFTR NBD1 and modeled (human) CFTR NBD2 structures, 1.48 Å and 1.49 Å, respectively (342 and 344 superimposed Cα atoms); (iii) between the observed human TAP1 and the modeled human CFTR NBD1 and NBD2 structures, 1.23 Å and 1.27 Å, respectively (382 and 398 superimposed Cα atoms). Next, for the construction of the CFTR NBD1/NBD2 heterodimer, we used, however, the CFTR NBD1 model (which allows the formation of an interface with NBD2) instead of the experimental mouse or human NBD1 structures. Indeed, these experimental structures harbor regions, RI and the regulatory extension (RE) [9, 10], which interfere with the formation of the NBD1/NBD2 heterodimer. These regions were either observed in a wrong place because of intermolecular interactions in the crystal lattice or they have to move out of the way via a conformational change before dimerization can occur. Anyway, these regulatory segments appear to be conformationally mobile, as they have been observed in different positions in the human and mouse CFTR NBD1 experimental structures [9, 10]. Worth noting in our model is the presence of the stacking interaction between W401 and the ATP adenine, in a conformation usually observed in head-to-tail NBD dimers (see fig. 4). It should also be stressed that all the observations made for amino acids belonging to NBD1 were supported by the identification of similar properties on the NBD1 experimental

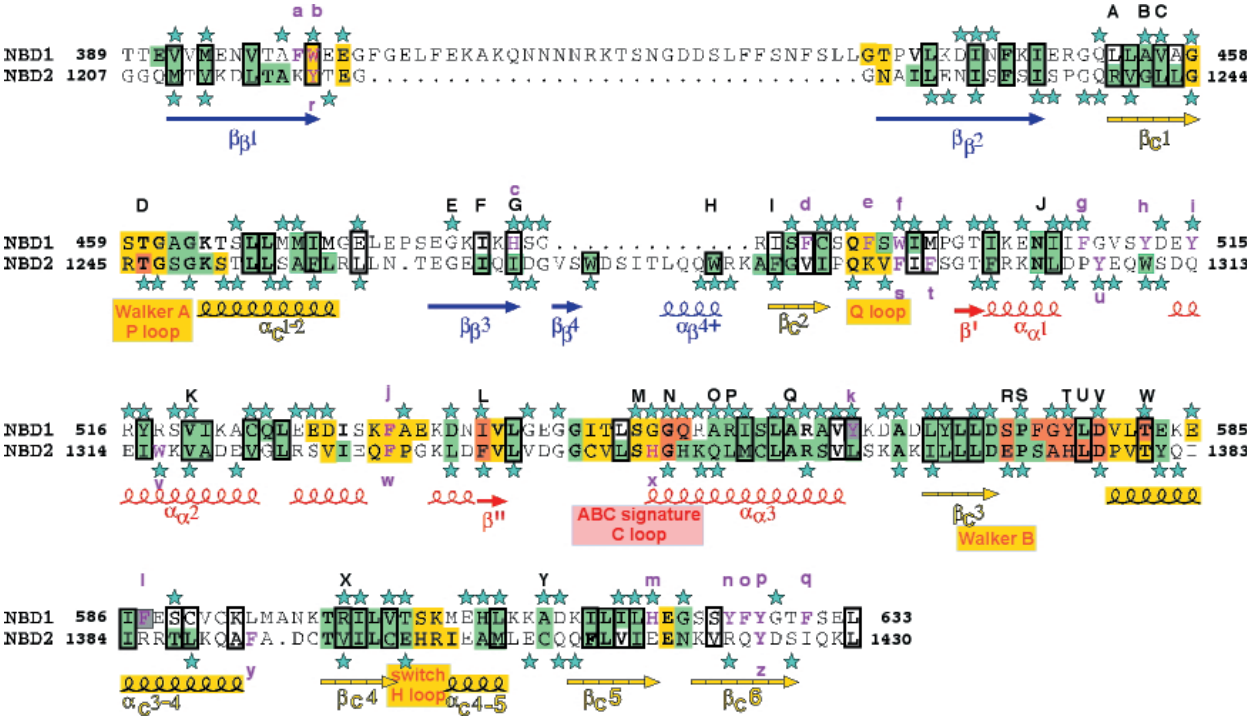

Figure 2. Alignment of the sequences of the two NBDs of human CFTR. Positions of the secondary structures are indicated below the alignment (labeling as in Callebaut et al. [11]). Buried amino acids are shaded green, those occupying topohydrophobic positions being boxed. Topohydrophobic positions were defined from a multiple alignment of divergent sequences (see fig. 1 in Callebaut et al. [11]) as those which are mainly occupied by hydrophobic amino acids (V, I, L, F, M, Y, W). Amino acids for which a difference in solvent accessibility was observed between the isolated NBD subunit and the NBD1/NBD2 heterodimer complex are mostly located at the interface between the NBDs and are shaded yellow or orange. Amino acids in orange are solvent-accessible when considering the isolated NBD subunit and buried within the heterodimer, whereas amino acids in yellow correspond to exposed residues for which only a variation in solvent accessibility was observed. Aromatic amino acids which are accessible to solvent are indicated in pink and labeled with small letters from a to z (a to q for NBD1, r to z for NBD2). Residues F587 and Y563, whose side chain accessibility may be due to a modeling artifact (see text and fig. 6) are shaded gray. All other amino acids discussed in the text are labeled with capital letters from A to Y (whatever the concerned NBD). Amino acids, for which a mutation has been reported in the CFTR mutation database (http://www.genet.sickkids.on.ca/cftr), are indicated by stars.

structures (except for Y563 and F587, two exposed aromatic residues, which are further discussed below in the Results and discussion section). Here, labeling of the secondary structures is as in the MJ0796 structure [13] and in our model reported previously [11], the subscript indicating the subdomain in which the secondary structure is located (α-, β-specific subdomains or c for core subdomain). Topohydrophobic positions [22] were defined as positions for which, in multiple sequence and/or structure-based alignments (necessarily including divergent sequences), hydrophobicity is a conserved character. In the present work, they have been deduced after superimposition of the known experimental structures of eight ABC transporter NBDs sharing low sequence identity. Three-dimensional structures were manipulated using Swiss-PDB Viewer [23]. The solvent-accessible surfaces of the amino acid residues were calculated using DSSP [24], a cut-off value of 10% of relative accessibility being used for the identification of amino acids buried in the interior of the molecule. Identification of the regions for which discordances can be observed between their predicted and experimental secondary structures was performed using an original in-house program [R. Eudes et al., unpublished results]. Briefly, our DISCORDANCE program compares the observed secondary structures – as defined by a consensus of different assignment methods starting from atomic coordinates (DSSP [25], Define [26], STRIDE [27], P-SEA [28]) – to the secondary structures predicted by the PSI-PRED program, on the basis of the sequence [29]. Finally, the Hydrophobic Cluster Analysis (HCA) method [30, 31] was used to investigate further the possible local conformation of the $\alpha_\alpha 1$–$\alpha_\alpha 2$ segment of the NBDs. Guidelines to the use of this method were previously outlined [11, 30, 31].

Results and discussion

To gain some insight into the potential effects of human CFTR NBD mutations from a structural point of view, we first performed an analysis of the solvent-accessible

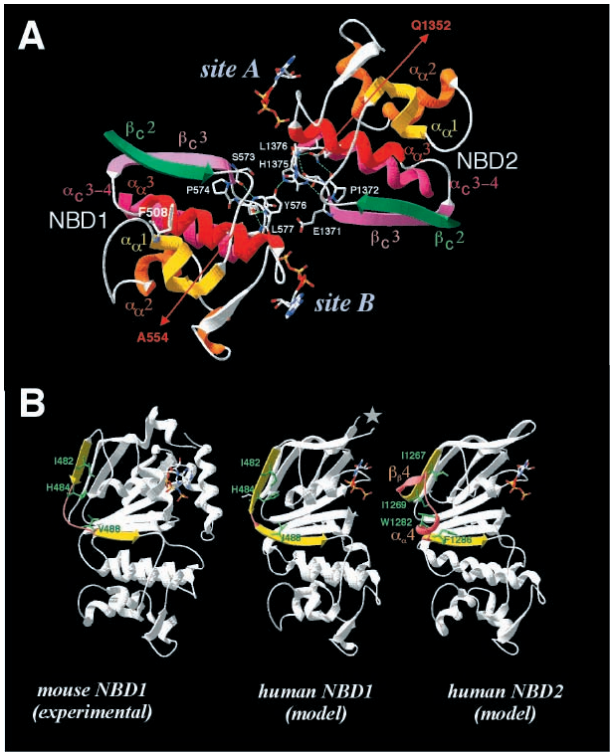

Figure 3. Insights into critical positions buried within the CFTR NBD1/NBD2 heterodimer. (A) A554 in NBD1 and its corresponding residue Q1312 in NBD2. (B) Buried positions which are specific to CFTR NBD2.

surface not only of the NBD1/NBD2 heterodimer model, but also of each NBD subunit considered individually. Indeed, this allowed us to discriminate between amino acids buried in the interior of the molecule, the alteration of which might affect folding and stability of the domain, and amino acids located on the surface and thereby possibly exposed to the solvent, which might rather be involved in functional aspects (e. g. interactions with other domains) and/or protein solubility. Of note, amino acids involved in the active sites (ATP binding and hydrolysis) are localized at the interface between the two heterodimer subunits and can thus be regarded both as exposed when considering an isolated subunit and as buried (or partially buried) when considering the dimerized structure. Thus, we hereafter describe successively each of these three structural classes of amino acid positions, with emphasis on some mutations described in CF patients (black and pink letters in fig. 2). First, we will deal with buried amino acids, before considering residues localized at the heterodimer interface, in particular, active-site residues. We next discuss the case of exposed amino acids located on the surface of the heterodimer considered alone and finally conclude by suggesting some novel features involving potential conformational mobility within the CFTR NBD subunits. The data presented here are also summarized in a table provided as supplementary material (http://www.lmcp.jussieu.fr/~mornon/CFTR-table.html).

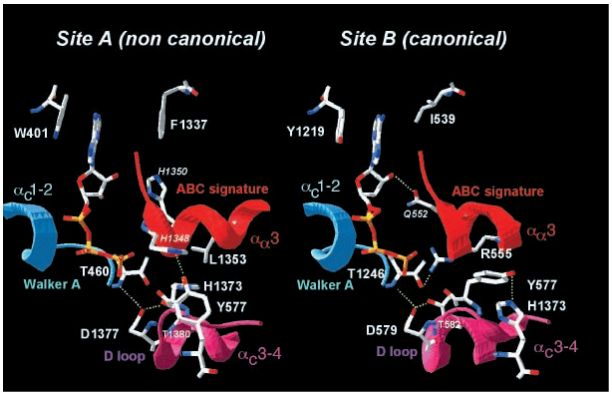

Figure 4. View of the two nucleotide-binding sites after their superimposition. Only a few particular amino acids, which are discussed in the text, are shown in atomic detail. These residues, which are mainly located outside the ABC conserved motifs are, however, noticeable as they participate in the heterodimer interface. The Cα traces of the Walker A motif (P-loop), ABC signature and D-loop (located just after the Walker B motif) are shown in a ribbon representation.

Amino acids buried in the interior of the CFTR NBD domains. Buried amino acids are depicted on a green background in figure 2. They are generally non-polar and often occupy "topohydrophobic" positions (i. e. sites which, in a multiple alignment of a family of sequences, are mainly occupied by highly hydrophobic residues) [22]. These topohydrophobic positions are boxed in figure 2 and are generally crucial for fold stability [22, 32]. Among the mutations which have been described in CF patients (indicated by stars in fig. 2), several affect amino acid residues occupying such buried topohydrophobic positions and the resulting modification can be expected to alter the fold of the NBDs. Examples are V456F [33] and V520F [34] (labeled C and K, respectively, in fig. 2) which involve residues buried in the interior of the NBD1 subdomain. A few topohydrophobic positions appear, however, exposed to the solvent (boxed and non-green shaded amino acids in fig. 2), and are therefore expected to play a particular role in the interactions of the NBD domains with the other domains of CFTR or even with CFTR partners (see below).

On the other hand, topohydrophobic positions can occasionally be occupied by non-hydrophobic amino acids. For example, this is the case for NBD2 R1239 (aligned with NBD1 L453, labeled A in fig. 2). Interestingly, it appears that the long aliphatic side chain of this amino acid may form a hydrophobic contact with the side chain of C1410, localized in a position occupied in other ABC NBDs by a small apolar residue. Another example is NBD1 R600 (aligned with NBD2 V1397, mutated in CF [35], labeled X in fig. 2), with its polar extremity pointing toward the solvent, whereas the equivalent position in other NBDs is occupied by hydrophobic amino acids, which have smaller side chains and are consequently fully buried.

Some buried amino acids do not occupy topohydrophobic positions (green shaded but not boxed amino acids in fig. 2). Noticeable examples are A554 in CFTR NBD1 and Q1352 in CFTR NBD2 (labeled O in fig. 2), the last one having been found mutated in CF [36]. Amino acids at this position in helix $\alpha_\alpha 3$ (labeling of secondary structures as reported in the MJ0796 structure [13] and in our model [11]) are highly conserved in ABC NBDs and often correspond to a glutamine residue. The glutamine side chain indeed forms a tight network of hydrogen bonds with the main chain of residues (P1372, L1376, labeled S and U in fig. 2) located in the $\beta_c 3$–$\alpha_c 3$-4 loop, which participates in both active sites of the heterodimer (fig. 3A). This network might contribute to the appropriate conformation of the catalytic glutamate (E1371, labeled R in fig. 2) of the NBD2 Walker B motif, which is included in this loop and participates in the canonical active site B. In contrast, such a network cannot exist in NBD1, and thus in the non-canonical ATP-binding active site A, as the NBD1 residue corresponding to NBD2 Q1352 is an alanine (A554, labeled O in fig. 2; fig. 3A). A similar role in forming an appropriate network of H bonds for the stabilization of the γ-phosphate linker (Q-loop) can be predicted for the buried asparagine residues located within helix $\alpha_\alpha 1$ (NBD1 N505 and NBD2 N1303, labeled J in fig. 2) [37].

Several class II mutations (defective CFTR folding and trafficking), such as the relatively frequent N1303K mutation (labeled J in fig. 2), involve buried residues (fig. 1). Other examples (fig. 1) are: (i) A455E [38–40] (labeled B in fig. 2); (ii) P574H [40, 41] (labeled S in fig. 2); (iii) A559T [42, 43] (labeled Q in fig. 2). Worth noting is that A455E and P574H are mild alleles, as they have been found associated with preserved pancreatic function and residual secretion of chloride; in addition, a correlation between the A455E mutation and mild pulmonary disease has also been reported [38]. Thus, although these mutations involve residues buried within NBD1, they may only lead to limited impairment of the co-translational NBD1 folding. Accordingly, the missense mutation V456F (labeled C in fig. 2), which involves a topohydrophobic position buried in NBD1 (see above), was also reported in a patient suffering from a mild (pancreas-sufficient) form of CF [33]. Taken together, these considerations suggest that class II mutations involving buried residues may in some instances lead to relatively mild forms of CF disease. However, the N1303K mutation (labeled J in fig. 2), which involves a position buried in NBD2, was classified not as a mild, but as a severe mutation [44]. This substitution may actually affect not only the folding of the subunit, but also the ATPase activity, as N1303 is directly involved in the stabilization of the NBD2 Q-loop (see above).

Interestingly, ΔF508 is also a class II mutation. However, F508 (labeled g in fig. 2) is not buried within the NBD heterodimer, but exposed at the surface of the NBD1 subunit (see below). It has recently been shown that mutations and deletion of this residue cause in fact only limited alteration of the NBD1 conformation [10, 19] but impair the native interaction of NBD2 with NBD1 [45] and the post-translational folding of the full-length CFTR protein [19]. Thus, class II mutations appear to affect either the folding or fold stability of individual subunits (buried residues) or the domain-domain assembly and overall folding of the entire protein (exposed residues). An important role in signaling with the MSDs can thus be expected for the F508 residue (see below). Such an important functional role might actually explain the class III phenotype shown by ΔF508 when rescued (for example, at low temperature). Another class II mutation, G480C, involves a non-buried position (labeled E in fig. 2). Similarly to ΔF508, the G480C mutant has been found to be defective in its intracellular processing and to exhibit chloride channel properties when allowed to traffic in *Xenopus* oocytes [46]. This mutation possibly also impairs the domain-domain assembly of CFTR. We should also stress here that both ΔF508 and G480C, which are class II mutations affecting residues possibly involved in domain-domain interactions, are considered as clinically severe mutations. Accordingly, mouse models carrying the severe ΔF508 and G480C mutations have been generated to provide valuable in vivo systems to test novel therapeutic approaches [47].

Finally, some buried positions are found only in NBD2, as shown by our model and the experimental structure of mouse CFTR NBD1 (fig. 3B). Indeed, CFTR NBD1 lacks strand $\beta_\beta 4$ and helix $\alpha_\beta 4$, which are present in the other NBDs of known structure. Consequently, some hydrophobic amino acids are exposed in NBD1 (I482, H484, I488; labeled F, G and I in fig. 2), whereas the corresponding residues are buried in NBD2 via these secondary structures (I1267, I1269, F1286). Other residues, which belong to the NBD2-specific secondary structures mentioned above (W1282; labeled H in fig. 2), are obviously not present in NBD1 (fig. 3B).

Amino acids at NBD1/NBD2 interface. Amino acids participating in the interface can be described as those for which a significant difference in solvent accessibility is observed between the isolated structure of the corresponding subunit (without ATP) and the heterodimer structure. These residues are shaded yellow and orange in figure 2. The orange color indicates amino acids which are exposed on the surface of the isolated NBD structure but buried within the heterodimer complex, whereas residues in yellow have only a lower solvent accessibility (but remain, however, exposed) in the heterodimer. Such a varying solvent accessibility was generally found for equivalent positions in the two subunits. A few positions were however specific to a given subunit and could be cor-

related with the asymmetric structure of the heterodimer. As expected from known ABC head-to-tail architectures [6, 12, 13], in particular that of the MJ0796 dimer which was used as template for modeling [13], amino acid residues located in highly conserved motifs of the NBD domains (Walker A, Walker B, H-loop, Q-loop and ABC signature) participate either in ATP binding or in the direct interaction between NBD1 and NBD2 at their interface, as already discussed previously [11]. Particularly worth noting here is that most of the class III mutations (affecting Cl^- channel gating) involve residues located within the NBD active sites. The most striking example is the G551D missense mutation (labeled N in fig. 2) which involves a residue located in the LSGGQ motif of the NBD1 ABC signature of the conventional ATP-binding site B (fig. 1). A mouse model of this human mutation of particular interest has been created to enable the pre-clinical testing of mutation-specific therapeutic approaches [48]. Interestingly, in CF patients, the defective function of the appropriately localized G551D protein could be rescued by genistein [49]. This CFTR activator has recently been proposed to bind in a cavity at the interface between the subunits, and to have close contacts with the Walker A, LSGGQ signature and Walker B motifs of NBD1 and, to a lesser extent, with the LSHGH signature motif of NBD2 [50]. However, S549R (labeled M in fig. 2), which also involves a residue of the NBD1 ABC signature participating in the binding of the ATP γ-phosphate in the conventional site B, was identified as a class II mutation (fig. 1). This may be related to a structural role of S549 in the folding itself of NBD1 (or even NBD2) in addition to its role in ATP binding.

In the present work, we especially focused our analysis on positions located outside the aforementioned conserved motifs, in order to unveil novel specific features of the CFTR NBD interface. This led us to describe here the features of a series of corresponding amino acid residues (which are depicted in fig. 4).

i) R555/L1353 (labeled P in fig. 2). These amino acids are located in helix $\alpha_\alpha 3$ of NBD1 and NBD2, respectively. Their aliphatic chains are buried within the core of their respective subunits. Only the charged end of R555 points toward the solvent in the isolated structure of NBD1, whereas L1353 is fully buried. In the heterodimeric structure, the side chain of R555 appears to form a hydrogen bond with that of T1246 (labeled D in fig. 2), reinforcing thereby the interface interaction at the level of the canonical site B, whereas such a bond can obviously not exist in the non-canonical site A. A similar situation was observed in the MJ0796 homodimer structure, where the conserved arginine (R153) interacts with S40 in the opposite subunit. Interestingly, an energetic coupling between CFTR NBD1 R555 and NBD2 T1246, which changes in concert with the channel gating status, has recently been reported [51]. In addition, R555 has previously been shown to be involved in the endoplasmic reticulum quality control mechanism and mutation of this residue into lysine was found to partially correct the defective processing of CFTR-ΔF508 [52, 53]. Thus, like the G550E mutation affecting the NBD1 ABC signature [54], a R555 mutation may restore (to some extent) the interactions disrupted by the ΔF508 mutation.

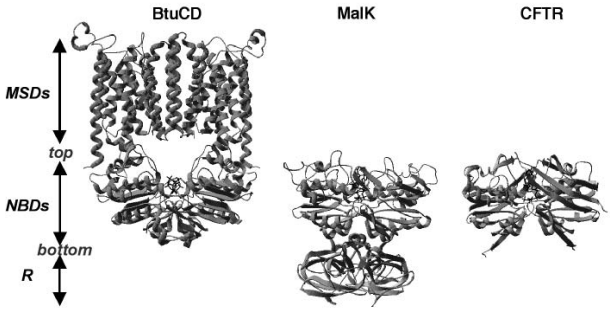

Figure 5. Lateral view of the structures formed by head-to-tail NBD dimers interacting with the other domains of the entire ABC protein. From left to right: (1) the transporter BtuCD, where the BtuD NBD homodimer (in complex with vanadate) interacts with the BtuC MSDs [6]; (2) the MalK homodimer (closed configuration, in complex with ATP) with its C-terminal regulatory domains [58]; (3) model of the human CFTR NBD1/NBD2 heterodimer (in complex with ATP) ([11] and this study).

ii) D579/D1377 (labeled V in fig. 2). D579 and its NBD2-equivalent D1377 correspond to the highly conserved aspartic acids of the D-loop, which are located just after the Walker B motif in the loop linking $\beta_c 3$ to helix $\alpha_c 3$-4. In MJ0796, the side chain of the corresponding aspartic acid (D177) forms hydrogen bonds with the main-chain amide of S40 in the opposite subunit. A similar situation was observed in the CFTR heterodimer in which the side chains of D579 and D1377 form hydrogen bonds with threonine residues located on the opposite subunit (T1246 and T460, respectively, labeled D in fig. 2). The D579G mutation has been observed in patients with pancreatic sufficiency and a mild pulmonary phenotype [55, 56].

iii) T582/T1380 (labeled W in fig. 2). These equivalent amino acids are located in the helix $\alpha_c 3$–4 and make a hydrogen bond with D579 and D1377 of the D loop, respectively (labeled V in fig. 2, see above). The T582R mutation is severe, with lung and pancreatic involvement [57].

iv) Y577/H1373 (labeled T in fig. 2). The position occupied by these two equivalent amino acids in the loop linking strand $\beta_c 3$ to helix$_c$3–4 is generally occupied in ABC domains by a small amino acid (such as alanine). Interestingly, as we have previously shown [11], the side chains of these amino acids might interact via a hydrogen bond, reinforcing thereby the dimerization. The Y577F mutation has been shown to be associated with severe lung disease and elevated sweat chloride levels (http://www.genet.sickkids.on.ca/cftr).

v) I539/F1337 (labeled L in fig. 2). F1337 is located upstream of the short strand β'' within the NBD2 α

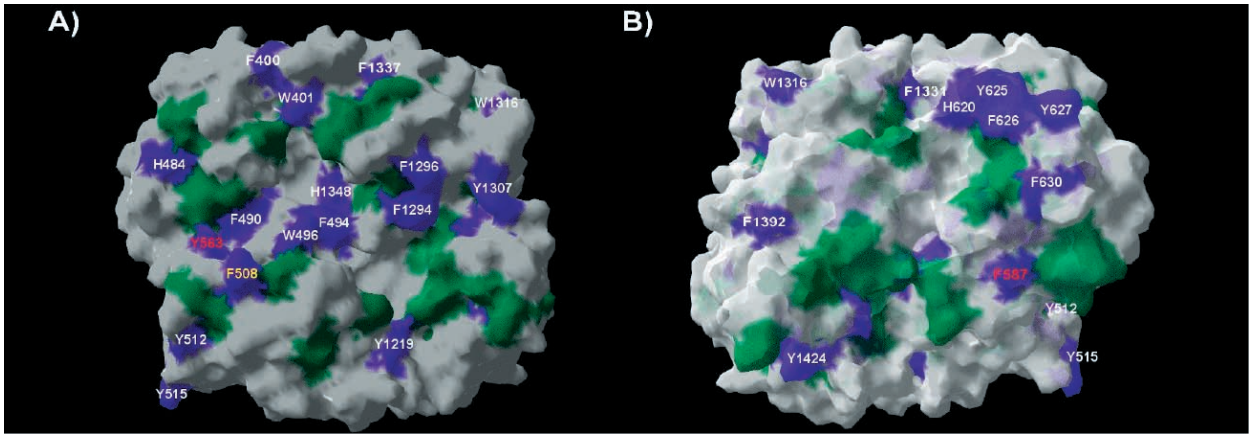

Figure 6. View of the solvent-accessible surface on the top (A) and bottom (B) sides of the CFTR NBD1/NBD2 heterodimer model. The solvent-accessible area formed by aromatic amino acids (tyrosine, phenylalanine, tryptophan, histidine) is shown in purple. Residue F508 is labeled in yellow, whereas residues F587 and Y563 (whose side chain accessibility may be due to a modeling artifact) are labeled in red. Solvent-accessible areas of other hydrophobic amino acids (valine, isoleucine, leucine, methionine, cysteine) are colored in green. The heterodimer is oriented as in figure 1. (A) Top side, likely in contact with the MSDs; (B) Bottom side, likely in contact with the regulatory R domain.

subdomain. In our model, this phenylalanine residue is oriented toward the dimer interface and might interact with the NBD1-specific insertion between strands $\beta_\beta 1$ and $\beta_\beta 2$ and thereby modulate the accessibility of active site A. The NBD1 equivalent position is occupied by an isoleucine (I539), the mutation of which was shown to rescue the processing and functional defects of CFTR ΔF508 [54].

vi) W401/Y1219 (labeled b and r, respectively, in fig. 2). As previously reported [11], there is a noticeable aromatic stacking interaction between the adenine of the nucleotides and W401 (site A) and Y1219 (site B), which are located at the end of strand $\beta_\beta 1$ of NBD1 and NBD2, respectively.

Aromatic amino acids exposed on the NBD1/NBD2 dimer surface. The global arrangement of ABC NBD dimers may be viewed as a somewhat flattened globular (pancake-like) structure with a top and a bottom surface, these two sides mediating the interactions with the other domains of the protein. Such a general scheme of interactions can indeed be deduced from observed three-dimensional configurations of ABC transporters in which the NBDs display a higher affinity for each other in the presence of the other domains (fig. 5). On the one hand, in the presence of the BtuC MSDs within the structure of the complete vitamin B12 transporter, the BtuD NBD head-to-tail homodimer has been shown to interact with the MSD intracellular loops via a top side involving its Q-loop and α subdomain [6]. On the other hand, as for the maltose transporter MalK, the additional regulatory domains located C-terminal to the NBDs (which dimerize in a head-to-tail configuration) have been observed to interact with the bottom side of the NBDs [58]. Helical structures linking the two domains are directly involved in the interaction.

A similar relative orientation may be expected for the MSDs and R domain of CFTR, although there are important differences between CFTR and the vitamin B12 and maltose transporters. First, the CFTR MSDs are composed of only six transmembrane helices, and not ten as in BtuC [6]. A comparison with the structures of MsbA [7, 8], which, like CFTR, has six transmembrane helices in its MSDs but for which the canonical head-to-tail arrangement of the NBDs is still being discussed [8, 59], led to the suggestion that the general mode of interaction between the NBDs and MSDs is conserved on the top NBD side of ABC transporters, always involving the Q-loop and helices from the α-subdomains. Second, as regards MalK, there is no readily detectable sequence similarity between its regulatory domain (which is present in two copies) and the CFTR R domain (which is present in a single copy and is connected to the N-terminal end of the second MSD). However, as in MalK, the CFTR R domain might be located on the same bottom side of the NBD dimer, as the C-terminal secondary structures ending the NBDs appear to be conserved between the different NBDs. The first helix located after the C-terminal $\beta_c 6$ strand of MalK can indeed be superimposed on that observed in the CFTR NBD1 experimental structure. Although the second helix in MalK occupies a different position to the extra helix in CFTR (considered to be part of the R domain), this additional extra helix may, as previously noticed [9], thrust directly into the opposite subunit (when modeling the CFTR NBD1/NBD2 heterodimer) and may be expected to move upon dimerization.

Along these lines, we calculated the solvent-accessible surface area of the CFTR NBD heterodimer model and identified aromatic amino acids exposed on its top and bottom sides (pink letters, labeled a to z in fig. 2). These residues may be valuable candidates for interacting with

the other CFTR domains. This led us to identify: (i) on the NBD1 surface (the labeling in figure 2 is as indicated between parentheses as follows): F400 (a), W401 (b), H484 (c), F490 (d), F494 (e), W496 (f); F508 (g); Y512 (h); Y515 (i); F533 (j), Y563 (k), F587 (l), H620 (m), Y625 (n), F626 (o), Y627 (p), F630 (q); (2) on the NBD2 surface: Y1219 (r), F1294 (s), F1296 (t), Y1307 (u), W1316 (v), F1331 (w), H1348 (x), F1392 (y); Y1424 (z).

Interestingly, on the top side (fig. 6A), which likely interacts with the MSDs, we observed a large cluster of aromatic amino acids straddling the two NBDs. It includes from the left to the right on figure 6A: Y563 (k in fig. 2), F508 (g), F490 (d), W496 (f), F494 (e), H1348 (x), F1294 (s), F1296 (t), Y1307 (u). Among these residues, F494, W496 and F508 (the most common CF mutation site) have already been identified by Lewis et al. [9] as candidates for the NBD1 interface with the MSD. We propose here that a similar, nearly symmetrical patch exists on the NBD2 top surface, both patches forming a continuous line crossing the NBD heterodimer. The potential of this aromatic stretch for interaction with the MSDs is supported by recent experimental data showing that ΔF508 causes limited alteration of the fold of the isolated NBD1 subunit [10, 19], but impairs interdomain interactions [45] and especially disrupts packing of the transmembrane segments [60]. Of note, the exposed behavior of the Y563 side chain may, however, be due to a modeling artifact as it is clearly more buried in the NBD1 experimental structures. Missense mutations affecting Y563 (Y563N, Y563D, Y563C) have been reported, reduced levels of mature CFTR being observed for Y563N [40]. This is thus another example of a class II mutation involving the substitution of a buried amino acid. In addition to the central three-dimensional alignment of exposed aromatic amino acids, we also found two other parallel alignments of hydrophobic amino acids (with either aliphatic or aromatic side chains), which might provide additional interaction with the MSDs. Aromatic amino acids belonging to these parallel alignments are: (i) at the corners: H484 (c in fig. 2), Y512 (h), Y515 (i) (NBD1) and W1316 (v) (NBD2); (ii) proximal to the ATP-binding sites: F400 (a) and W401 (b) (non-canonical site A) and Y1219 (r) (canonical site B). As already discussed above, W401 and Y1219 provide stacking interaction with the nucleotide adenine. Indeed, only a portion of the side chain of these residues is in fact exposed on the top side of the dimer, the other portion being involved in the stacking interaction at the heterodimer interface. Finally, stress that identical results were obtained for the solvent accessibility of the aromatic amino acids on the experimental structure of mouse and human CFTR NBD1 [9, 10].

On the bottom side of the NBD1/NBD2 heterodimer (fig. 6B), which is likely to interact with the CFTR R domain, only a few aromatic side chains may be exposed to the solvent: F587 (l in fig. 2), H620 (m), Y625 (n), F626

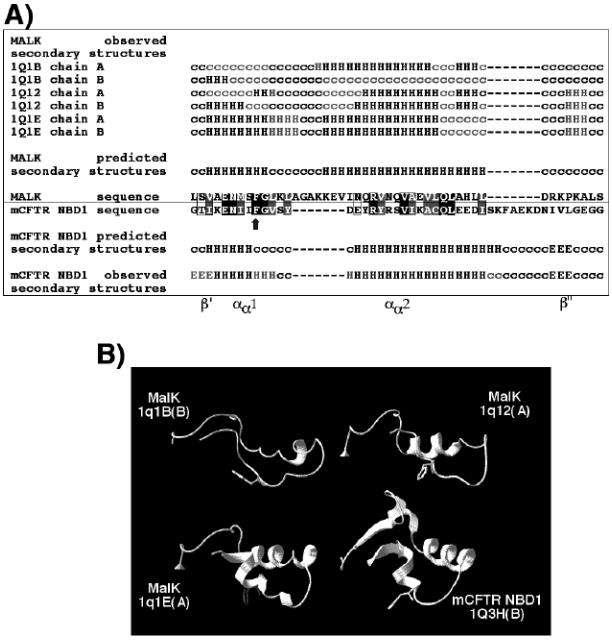

Figure 7. Discordances between the predicted (PSI-PRED program [29]) and experimentally observed secondary structures of the $\alpha_\alpha 1$–$\alpha_\alpha 2$ segment of the MalK NBD homodimer (with its chains A and B), suggesting that the equivalent CFTR NBD1 segment may undergo conformational changes. (A) Alignment of the MalK and mouse CFTR (mCFTR) sequences, the CFTR F508 residue being aligned with MalK F98 (arrow). Secondary structures are labeled H, E and c for helix, strand (extended) and coil, respectively. For MalK, the predicted secondary structures are compared with the secondary structures observed in three experimental dimers, discordances (shown in gray) being essentially noted in two cases (PDB identifiers 1Q1B and 1Q12 (closed dimer with ATP)) but not in the third one (PDB identifier 1Q1E). Also, no striking discordance can be noticed for mCFTR NBD1 (PDB identifier 1Q3H). (B) Ribbon representation of the NBD $\alpha_\alpha 1$ – $\alpha_\alpha 2$ segment of the three experimental MalK structures and of mCFTR NBD1, with the CFTR F508 and MalK F98 being shown in atomic details

(o), Y627 (p), F630 (q), F1331 (w), F1392 (y), Y1424 (z). However, the five amino acids located on $\beta_c 5$ (H620), $\beta_c 6$ (Y625, F626 and Y627) and on the $\beta_c 6/\alpha$-ter loop (F630) are buried in the experimental structure of mouse NBD1 as they are covered by the C-terminal helix, which was not modeled in our heterodimer. Y1424 is located in a position in NBD2 that is similar to that of Y627 in NBD1, and may thus also be buried by a C-terminal α helix. As for F587, its exposed nature might be due to a modeling artifact, as its side chain is more buried in the NBD1 experimental structures (as discussed above for residue Y563). It appears therefore that except for F533, F1331 and F1392, no other large aromatic patch is present on the bottom side of the CFTR NBD heterodimer. Noticeably, the location of the aromatic and hydrophobic amino acids on the bottom side is clearly more asymmetrical than on the top side. This may be related to the existence of two similar MSD domains interacting with the NBD subunits, in contrast to the unique R domain of CFTR.

Finally, although the most common CF mutation, ΔF508,

involves the exposed F508 residue, only a few missense mutations affecting these exposed aromatic residues have been reported: H484R, Y515H, H620P, H620Q and Y1307C (http://www.genet.sickkids.on.ca/cftr).

Insights into the potential conformational mobility of the NBD α subdomains. Conformational changes are believed to affect the positioning of the different domains of ABC transporters relative to each other, but they can also occur within a specific domain. In particular, as regards the NBDs, a rigid body rotation between the ATPase core and the α-helical subdomain has been described [21, 58, 61, 62]. This movement of the NBD α-helical subdomain, which depends on the type of nucleotide (ATP or ADP), is thought to play a critical role in signaling with the MSDs.

Besides rigid body movement, other critical conformational changes may involve a local refolding of the polypeptidic chain. Such mechanisms have been observed for example with the influenza virus hemagglutinin (coil to α transition) and with the prion protein (α to β transition). We [31, 63] and others [64, 65] have reported that segments susceptible to secondary-structure transition were detectable in several cases because the predicted secondary structures dramatically differed from the observed (likely metastable) states. We have thus analyzed all the known structures of ABC transporter NBDs in search of such discordant segments. This allowed us to identify a fragment of the *Escherichia coli* MalK transporter which was predicted to be a α helix but was observed as a coil in two experimental structures (fig. 7). This discordance did not however exist for a third experimental structure of the same transporter, in which the corresponding segment was observed in an α-helical conformation (as predicted). Such a discordant situation suggests that this fragment may undergo a conformational transition, a hypothesis strengthened by the observation of high temperature factors associated with this region in the crystal structure. Remarkably, this segment corresponds to helix $\alpha_\alpha 1$, which is predicted to interact with the MSDs and where the CFTR F508 residue is located. Worth noting is that there is a phenylalanine residue in the equivalent position in MalK and that the sequences of this region are particularly similar between the two proteins (fig. 7). One can also note that the hydrophobic cluster (defined using the HCA approach [30, 31]) which is associated with this segment, has an amino acid composition actually typical of a β strand, and not of an α helix. Taken together, these considerations suggest that this region may in fact alternate between extended β and helical α configurations. Interestingly, conformational changes in this region have also been proposed by molecular dynamics [66].

Conclusions. In the present work, we performed an in-depth analysis of our previously reported model of the human CFTR NBD1/NBD2 heterodimer to shed some light (at the molecular level) on the structural and/or functional role of various amino acids, in particular residues which have been found mutated in CF patients. Although predicting how a given mutation affects the protein structure/function is still quite difficult, especially on the basis of a static model, such a study is nevertheless potentially more informative than analysis of the simple protein sequence [67]. As in proteins associated with other inherited diseases, mutations in the CFTR NBDs appear to involve positions which are important for protein structure and function. They often involve residues which are highly conserved among different ABC proteins. Not surprisingly, mutations of residues buried within the interior of a NBD subdomain may affect its folding and consequently CFTR maturation. At the interface of the NBD1/NBD2 heterodimer, the NBD1 ABC signature and the NBD2 Walker A motif of the canonical ATP-binding site appear more prone to mutation than the corresponding motifs of the non-canonical ATP-binding site. Here, mutations of active-site residues are likely to affect activation of the channel via ATP. Our analysis also revealed the potential role of other interface residues in NBD1-NBD2 interaction. Amino acids exposed at the surface of the heterodimer may also play a highly critical role. They can indeed be involved in interdomain interactions and their mutation might thus impair the fold stability or folding and maturation of the entire CFTR protein. Such a role was recently demonstrated for the ΔF508 mutation and we suggest that a similar role may be expected for other amino acids such as G480. Finally, the two regions absent from of all other solved structures of NBDs, which were termed RI (residues 404 to 435) and RE (residues 639 to 670), contain only few CF mutations (see http://www.genet.sickkids.on.ca/cftr), which, moreover, do not affect the serine residues phosphorylated by protein kinase A (PKA) (S422, S659, S660, S670) [9]. Although a recent study reported that these non-conserved segments appear not essential for PKA- or ATP-dependent regulation of CFTR [68], mutations in these regions may have an effect on their conformational mobility and thereby affect heterodimer formation and stability. In conclusion, by highlighting the potential critical role of a series of amino acid residues of the NBD1/NBD2 human CFTR heterodimer, our work may pave the way for important site-directed mutagenesis studies in the future.

Acknowledgments. This work was supported by a fellowship (R. E.) and grants from the association Vaincre La Mucoviscidose (Paris, France).

1 Sheppard D. N. and Welsh M. J. (1999) Structure and function of the CFTR chloride channel. Physiol. Rev. **79:** S23–S45
2 Kidd J. F., Kogan I. and Bear C. E. (2004) Molecular basis for the chloride channel activity of cystic fibrosis transmembrane onductance regulator and the consequences of disease-causing mutations. Curr. Top. Dev. Biol. **60:** 215–249

3 Ostedgaard L. S., Baldursson O. and Welsh M. J. (2001) Regulation of the cystic fibrosis transmembrane conductance regulator Cl^- channel by its R domain. J. Biol. Chem **276:** 7689–7692
4 Welsh M. J. and Smith A. E. (1993) Molecular mechanisms of CFTR chloride channel dysfunction in cystic fibrosis. Cell **73:** 1251–1254
5 Schmitt L. and Tampe R. (2002) Structure and mechanism of ABC transporters. Curr. Opin. Struct. Biol. **12:** 754–760
6 Locher K. P., Lee A. T. and Rees D. C. (2002) The *E. coli* BtuCD structure: a framework for ABC transporter architecture and mechanism. Science **296:** 1091–1098
7 Chang G. and Roth C. B. (2001) Structure of MsbA from *E. coli*: a homolog of the multidrug resistance ATP binding cassette (ABC) transporters. Science **293:** 1793–1800
8 Chang G. (2003) Structure of MsbA from Vibrio cholera: multidrug resistance ABC transporter homolog in a closed conformation. J. Mol. Biol. **330:** 419–430
9 Lewis H. A., Buchanan S. G., Burley S. K., Conners K., Dickey M., Dorwart M. et al. (2004) Structure of nucleotide-binding domain 1 of the cystic fibrosis transmembrane conductance regulator. EMBO J. **23:** 282–293
10 Lewis H. A., Zhao X., Wang C., Sauder J. M., Rooney I., Noland B. W. et al. (2005) Impact of the DeltaF508 mutation in first nucleotide-binding domain of human cystic fibrosis transmembrane conductance regulator on domain folding and structure. J. Biol. Chem. **280:** 1346–1353
11 Callebaut I., Eudes R., Mornon J. P. and Lehn P. (2004) Nucleotide-binding domains of human cystic fibrosis transmembrane conductance regulator: detailed sequence analysis and three-dimensional modeling of the heterodimer. Cell. Mol. Life Sci. **61:** 230–242
12 Hopfner K. P., Karcher A., Shin D. S., Craig L., Arthur L. M. and Carney J. P. (2000) Structural biology of Rad50 ATPase: ATP-driven conformational control in DNA double-strand break repair and the ABC-ATPase superfamily. Cell **101:** 789–800
13 Smith P. C., Karpowich N., Millen L., Moody J. E., Rosen J., Thomas P. J. et al. (2002) ATP binding to the motor domain of an ABC transporter drives formation of a nucleotide sandwich dimer. Mol. Cell **10:** 139–149
14 Higgins C. F. and Linton K. J. (2004) The ATP switch model for ABC transporters. Nat. Struct. Mol. Biol. **11:** 918–926
15 Kidd J. F., Ramjeesingh M., Stratford F., Huan L. J. and Bear C. E. (2004) A heteromeric complex of the two nucleotide binding domains of cystic fibrosis transmembrane conductance regulator (CFTR) mediates ATPase activity. J. Biol. Chem. **279:** 41664–41669
16 Aleksandrov L., Aleksandrov A., Chang X.-B. and Riordan J. R. (2002) The first nucleotide binding domain of cystic fibrosis transmembrane conductance is a site of stable nucleotide interaction, whereas the second is a site of rapid turnover. J. Biol. Chem. **277:** 15419–15425
17 Basso C., Vergani P., Nairn A. C. and Gadsby D. C. (2003) Prolonged nonhydrolytic interaction of nucleotide with CFTR's NH2-terminal nucleotide binding domain and its role in channel gating. J. Gen. Physiol. **122:** 333–348
18 Berger A. L., Ikuma M. and Welsh M. J. (2005) Normal gating of CFTR requires ATP binding to both nucleotide-binding domains and hydrolysis at the second nucleotide-binding domain. Proc. Natl. Acad. Sci. USA **102:** 455–460
19. Thibodeau P. H., Brautigam C. A., Machius M. and Thomas P. J. (2005) Side chain and backbone contributions of Phe508 to CFTR folding. Nat. Struct. Mol. Biol. **12:** 10–16
20 Rowntree R. K. and Harris A. (2003) The phenotypic consequences of CFTR mutations. Ann. Hum. Genet. **67:** 471–485
21 Gaudet R. and Wiley D. C. (2001) Structure of the ABC ATPase domain of human TAP1, the transporter associated with antigen processing. EMBO J. **20:** 4964–4972
22 Poupon A. and Mornon J. P. (1998) Populations of hydrophobic amino acids within protein globular domains: identification of conserved topohydrophobic positions. Proteins **33:** 329–342
23 Guex N. and Peitsch M. C. (1997) SWISS-MODEL and the Swiss-PdbViewer: an environment for comparative protein modeling. Electrophoresis **18:** 2714–2723
24 Holm L. and Sander C. (1991) Database algorithm for generating protein backbone and side-chain coordinates from a C-α trace: application to model building and detection of coordinates errors. J. Mol. Biol. **218:** 183–194
25 Kabsch W. and Sander C. (1983) Dictionary of protein secondary structure: pattern recognition of hydrogen-bonded and geometrical features. Biopolymers **22:** 2577–2637
26 Richards F. M. and Kundrot C. E. (1988) Identification of structural motifs from protein coordinate data: secondary structure and first-level supersecondary structure. Proteins **3:** 71–84
27 Frishman D. and Argos P. (1995) Knowledge-based protein secondary structure assignment. Proteins **23:** 566–579
28 Labesse G., Colloc'h N., Pothier J. and Mornon J. (1997) P-SEA: a new efficient assignment of secondary structure from C alpha trace of proteins. Comput. Appl. Biosci. **13:** 291–295
29 Jones D. T. (1999) Protein secondary structure prediction based on position-specific scoring matrices. J. Mol. Biol. **292:** 195–202
30 Gaboriaud C., Bissery V., Benchetrit T. and Mornon J. P. (1987) Hydrophobic cluster analysis: an efficient new way to compare and analyse amino-acid sequences. FEBS Lett. **224:** 149–155
31 Callebaut I., Labesse G., Durand P., Poupon A., Canard L., Chomilier J. et al. (1997) Deciphering protein sequence information through hydrophobic cluster analysis (HCA): current status and perspectives. Cell. Mol. Life Sci. **53:** 621–645
32 Poupon A. and Mornon J. P. (1999) Predicting the protein folding nucleus from a sequence. FEBS Lett. **452:** 283–289
33 Dork T., Fislage R., Neumann T., Wulf B. and Tummler B. (1994) Exon 9 of the CFTR gene: splice site haplotypes and cystic fibrosis mutations. Hum. Genet. **93:** 67–73
34 Jones C. T., McIntosh I., Keston M., Ferguson A. and Brock D. J. (1992) Three novel mutations in the cystic fibrosis gene detected by chemical cleavage: analysis of variant splicing and a nonsense mutation. Hum. Mol. Genet. **1:** 11–17
35 Petreska L., Koceva S., Gordova-Muratovska A., Nestorov R. and Efremov G. D. (1994) Identification of two new mutations (711 +3A→G and V1397E) in CF chromosomes of Albanian and Macedonian origin. Hum. Mol. Genet. **3:** 999–1000
36 Lee J. H., Choi J. H., Namkung W., Hanrahan J. W., Chang J., Song S. Y. et al. (2003) A haplotype-based molecular analysis of CFTR mutations associated with respiratory and pancreatic diseases. Hum. Mol. Genet. **12:** 2321–2332
37 Berger A. L., Ikuma M., Hunt J. F., Thomas P. J. and Welsh M. J. (2002) Mutations that change the position of the putative γ-phosphate linker in the nucleotide binding domain of CFTR alter channel gating. J. Biol. Chem. **277:** 2125–2131
38 Gan K. H., Veeze H. J., Ouweland A. M. van den, Halley D. J., Scheffer H., Hout A. van der et al. (1995) A cystic fibrosis mutation associated with mild lung disease. N. Engl. J. Med. **333:** 95–99
39 De Braekeleer M., Allard C., Leblanc J. P., Simard F. and Aubin G. (1997) Genotype-phenotype correlation in cystic fibrosis patients compound heterozygous for the A455E mutation. Hum. Genet. **101:** 208–211
40 Van Oene M., Lukacs G. L. and Rommens J. M. (2000) Cystic fibrosis mutations lead to carboxyl-terminal fragments that highlight an early biogenesis step of the cystic fibrosis transmembrane conductance regulator. J. Biol. Chem. **275:** 19577–19584
41 Ostedgaard L. S., Zeiher B. and Welsh M. J. (1999) Processing of CFTR bearing the P574H mutation differs from wild-type and deltaF508-CFTR. J. Cell. Sci. **112:** 2091–2098
42 McDowell T., Shackleton S., Dear S., Stroobant J. and Harris A. (1995) A cystic fibrosis patient who is homozygous for the A559T mutation. Am. J. Hum. Genet. **57:** 734
43 Gregory R. J., Rich D. P., Cheng S. H., Souza D. W., Paul S., Manavalan P. et al. (1991) Maturation and function of cystic fibrosis transmembrane conductance regulator variants bearing

mutation in putative nucleotide-binding domains 1 and 2. Mol. Cell. Biol. **11:** 3886–3893
44 Osborne L., Santis G., Schwarz M., Klinger K., Dork T., McIntosh I. et al. (1992) Incidence and expression of the N1303K mutation of the cystic fibrosis (CFTR) gene. Hum. Genet. **89:** 653–658
45 Du K., Sharma M. and Lukacs G. L. (2005) The DeltaF508 cystic fibrosis mutation impairs domain-domain interactions and arrests post-translational folding of CFTR. Nat. Struct. Mol. Biol. **12:** 17–25
46 Smit L. S., Strong T. V., Wilkinson D. J., Macek M., Mansoura M. K., Wood D. L. et al. (1995) Missense mutation (G480C) in the CFTR gene associated with protein mislocalization but normal chloride channel activity. Hum. Mol. Genet. **4:** 269–273
47 Scholte B. J., Davidson D. J., Wilke M. and De Jonge H. R. (2004) Animal models of cystic fibrosis. J. Cyst. Fibros. **3:** 183–190
48 Delaney S. J., Alton E. W., Smith S. N., Lunn D. P., Farley R., Lovelock P. K. et al. (1996) Cystic fibrosis mice carrying the missense mutation G551D replicate human genotype-phenotype correlations. EMBO J. **15:** 955–963
49 Illek B., Zhang L., Lewis N. C., Moss R. B., Dong J. Y. and Fischer H. (1999) Defective function of the cystic fibrosis-causing missense mutation G551D is recovered by genistein. Am. J. Physiol. **277:** C833–C839
50 Moran O., Galietta L. J. V. and Zegarra-Moran O. (2005) Binding of activators of the cystic fibrosis transmembrane conductance regulator in the nucleotide binding domains. Cell. Mol. Life Sci. **62:** 446–460
51 Vergani P., Lockless S. W., Nairn A. C. and Gadsby D. C. (2005) CFTR channel opening by ATP-driven tight dimerization of its nucleotide-binding domains. Nature **433:** 876–880
52 Teem J. L., Carson M. R. and Welsh M. J. (1996) Mutation of R555 in CFTR-delta F508 enhances function and partially corrects defective processing. Receptors Channels **4:** 63–72
53 Chang X.-B., Cui L., Hou Y.-x., Jensen T. J., Aleksandrov A. A., Mengos A. et al. (1999) Removal of multiple arginine-framed trafficking signals overcomes misprocessing of ΔF508 CFTR present in most patients with cystic fibrosis. Mol. Cell. **4:** 137–142
54 DeCarvalho A. C. V., Gansheroff L. J. and Teem J. L. (2002) Mutations in the nucleotide binding domain 1 signature motif region rescue processing and functional defects of cystic fibrosis transmembrane conductance regulator delta f508. J. Biol. Chem. **277:** 35896–35905
55 Picci L., Cameran M., Olante P., Zacchello F. and Scarpa M. (1999) Identification of a D579G homozygote cystic fibrosis patient with pancreatic sufficiency and minor lung involvement. Hum. Mutat. **13:** 173
56 Salvatore D., Tomaiuolo R., Abate R., Vanacore B., Manieri S., Mirauda M. P. et al. (2004) Cystic fibrosis presenting as metabolic alkalosis in a boy with the rare D579G mutation. J. Cyst. Fibros. **3:** 135–136
57 Casals T., Ramos M. D., Gimenez J., Larriba S., Nunes V. and Estivill X. (1997) High heterogeneity for cystic fibrosis in Spanish families: 75 mutations account for 90% of chromosomes. Hum. Genet. **101:** 365–370
58 Chen J., Lu G., Lin J., Davidson A. L. and Quiocho F. A. (2003) A tweezers-like motion of the ATP-binding cassette dimer in ABC transport cycle. Mol. Cell. **12:** 651–661
59 Jones P. M. and George A. M. (2004) The ABC transporter structure and mechanism: perspectives on recent research. Cell. Mol. Life Sci. **61:** 682–699
60 Chen E. Y., Bartlett M. C., Loo T. W. and Clarke D. M. (2004) The DeltaF508 mutation disrupts packing of the transmembrane segments of the cystic fibrosis transmembrane conductance regulator. J. Biol. Chem. **279:** 39620–39627
61 Yuan Y.-R., Blecker S., Martsinkevich O., Millen L., Thomas P. J. and Hunt J. F. (2001) The crystal structure of the MJ0796 ATP-binding cassette. J. Biol. Chem. **276:** 32313–32321
62 Verdon G., Albers S. V., Dijkstra B. W., Driessen A. J. and Thunnissen A. M. (2003) Crystal structures of the ATPase subunit of the glucose ABC transporter from Sulfolobus solfataricus: nucleotide-free and nucleotide-bound conformations. J. Mol. Biol. **330:** 343–358
63 Mornon J. P., Prat K., Dupuis F., Boisset N. and Callebaut I. (2002) Structural features of prions explored by sequence analysis. II. A PrP(Sc) model. Cell. Mol. Life Sci. **59:** 2144–2154
64 Kallberg Y., Gustafsson M., Persson B., Thyberg J. and Johansson J. (2001) Prediction of amyloid fibril-forming proteins. J. Biol. Chem. **276:** 12945–12950
65 Dima R. I. and Thirumalai D. (2002) Exploring the propensities of helices in PrP(C) to form beta sheet using NMR structures and sequence alignments. Biophys. J. **83:** 1268–1280
66 Jones P. M. and George A. M. (2002) Mechanism of ABC transporters: a molecular dynamics simulation of a well characterized nucleotide-binding subunit. Proc. Natl. Acad. Sci. USA **99:** 12639–12644
67 Steward R. E., MacArthur M. W., Laskowski R. A. and Thornton J. M. (2003) Molecular basis of inherited diseases: a structural perspective. Trends Genet. **19:** 505–513
68 Csanady L., Chan K. W., Nairn A. C. and Gadsby D. C. (2005) Functional roles of nonconserved structural segments in CFTR's NH2-terminal nucleotide binding domain. J. Gen. Physiol. **125:** 43–55